MAPPING OF COMPLEX VEGETATION COMMUNITIES AND SPECIES USING UAV-LIDAR METRICS AND HIGH-RESOLUTION OPTICAL DATA

Bikram Pratap Banerjee[1], Simit Raval[1], Patrick Joseph Cullen[2,3], Sarvesh Kumar Singh[1]

[1]School of Minerals and Energy Resources Engineering, University of New South Wales, Sydney, Australia NSW 2052
[2]School of Chemical Engineering, University of New South Wales, Sydney, Australia NSW 2052
[3]Department of Chemical and Environmental Engineering, University of Nottingham, UK

ABSTRACT

Mapping of sensitive species in environments such as upland swamps is important for management of anthropogenic impacts. However, the task is challenging due to the inherently complex distribution of species. Unmanned aerial vehicle (UAV) based remote sensing has the potential to map such complex environments. In this study, an integrated UAV and light detection and ranging (UAV-LiDAR) system was employed to map swamp and non-swamp vegetation in a complex upland swamp environment. The paper details the process of data acquisition, pre-processing, extraction of LiDAR metrics, dimensionality reduction, and different classification methods. Independent component analysis with support vector machine (ICA+SVM) produced the best classification results with a 69.9% overall accuracy (*OA*) and 0.62 kappa coefficient (*k*). The *OA* and *k* accuracy further improved to 73.6 % and 0.67 by adding high resolution optical (RGB) data along with the LiDAR data. The UAV-LiDAR technology offers an effective approach to distinguish between swamp and non-swamp vegetation communities.

Index Terms— UAV, LiDAR, classification, complex communities, upland swamps

1. INTRODUCTION

Upland swamps are uniquely diverse ecosystems comprising of treeless heaths and sedgelands. These highly sensitive and threatened ecosystems found in New South Wales, Australia are called the Temperate Highland Peat Swamps on Sandstone (THPSS) [1]. THPSS are characterised by the presence of specific vegetation species. It is therefore important to map the composition of vegetation communities in these environments at a fine spatial scale. Which is further important for the reconciliation of prevalent anthropogenic impacts (such as underground coal mining) on THPSS. Field-based ecological sampling has been the traditional approach [1], however this at times is difficult to perform due to the undulating terrain and dense bushy nature of the environment. A previous attempt, involving aerial and satellite-based methods, was limited to the delineation of the swamp boundaries and vegetation baseline [2]. Use of unmanned aerial vehicle (UAV) based optical and infrared cameras, improved the detection of a single species (*Gleichenia dicarpa*) [3] and mapping the boundaries of THPSS vegetation communities [4]. Recently, a preliminary study involving a UAV-hyperspectral system enabled mapping of five species (*Pteridium aqulinum, Allocasuarina littoralis, Empodisma minus, Lepidosperma limicola and Lepidosperma neesii*) [5]. In this study, for the first time a UAV based light detection and ranging (LiDAR) system was used to map swamp and non-swamp vegetation communities in a complex environment (THPSS).

2. MATERIALS AND METHODS

This section details the study area and ground truth campaign, the integrated UAV-LiDAR system (Fig. 1), mechanism of operation to collect data and processing steps to remove noise and to generate a classified output.

2.1. Study area and ground truth

The upland swamp study area is located near Wollongong, Australia (34º 21’ 24.0” S, 150º 51’ 51” E). The area consists of shrub type vegetation Thickets (Banksia and Tea Tree), and Sedgeland-Heath Complexes (Cyperoid, Restioid, and Sedgelands) [1, 5]. To simplify the classification, we narrowed the swamp type vegetation communities to; Sedgelands complex (*Empodisma minus, Lepidosperma limicola, Lepidosperma neesii, Leptocarpus tenax, and Gymnoschoenus sphaerocephalus, Schoenus brevifolius*) and species – Grass tree (*Xanthorrhoea resinosa*), Dagger Hakea (*Hakea teretifolia*), Pouched coral fern (*Gleichenia dicarpa*) and non-swamp trees – Eucalyptus and species – Black sheoak (*Allocasuarina littoralis*).

A rigorous ground truth collection campaign was performed. The study area was divided into two sites according to the UAV-flight plan (Fig. 2(a)). A total of 32 field sampling points were randomly targeted in Site-1 and 48 field points in Site-2. The locations were recorded using a ground-based real-time kinematic – differential global

positioning system (RTK-DGPS) with a Leica Viva GS15. Around each field sampling point, four observations were collected at 1 m distances in the North, East, South and West directions (with a compass to maintain bearing). Therefore, a total of (32+48) x 4 = 320 ground truth points were collected over the entire swamp area. Additionally, 128 ground truth polygons for the tree type vegetation were collected from high resolution (7.5 cm) image data (NearMap) acquired on the same date as the survey.

2.2. UAV-LiDAR acquisition

For this mission, we used a mobile LiDAR system (Phoenix Aerial Scout) integrated onto a customised hexa-copter UAV with a 3DR Pixhawk2 mini flight controller system. The system integration includes the mobile LiDAR sensor (Velodyne PUCK); onboard RTK-GPS unit; inertial measurement unit (IMU); embedded computer with onboard data storage unit; and Wi-Fi connection module (Fig. 1). The sensor records 0.3 million laser points per second on the onboard computer and downlinks a subsampled point cloud data to the ground station in real-time, through 5.8 GHz long-range Wi-Fi wireless system. The total system weighed under 9 kg and offered a flight time of around 15 minutes.

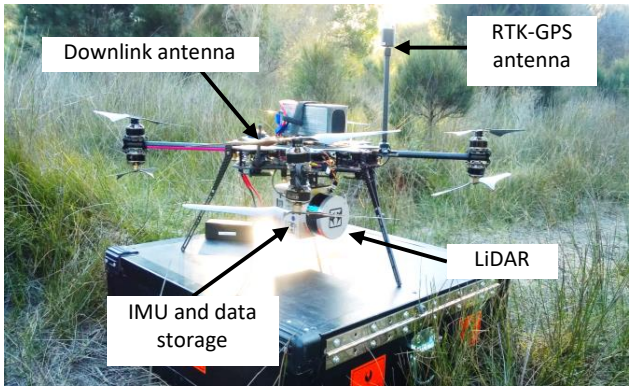

Fig. 1. The integrated UAV-LiDAR system in the study environment

The UAV-LiDAR system was operated over the two sites according to a pre-designed flight plan (Fig. 2(a)) with a flying height of 50 m and speed of 5 m/s, while keeping the transect spacing of 20 m.

2.3 Pre-processing

The following pre-processing steps were carried out on the raw UAV-LiDAR data:

Raw data to point cloud: along with the raw ranging information from the laser, the sensor records time-tagged roll, pitch, yaw and position information from the IMU and RTK-DGPS units. These raw datasets were fused to produce a point cloud (.las) file in Phoneix Aerial Spatial Fuser v3.0.5. The process included correction for the center of the IMU, RTK-DGPS to the laser sensor geometric translation. All 16 channels of the LiDAR were used for the generation of the point cloud. However, LiDAR returns with ranging values > 60 m were avoided in the process to keep the beam divergence within the limits. Furthermore, for the small intervals when the quality parameters were unsatisfactory (uncertainty in altitude > 0.1 m, position > 0.1 m, and number of available satellites < 9), fusion was avoided to achieve an accurate point cloud (rmse = 10 cm).

Subsampling: a LiDAR scan often contains closely placed redundant points, such points were removed by subsampling the data with a minimum threshold (th = 0.01 m) separation criterion.

Segmentation: LiDAR scans also produce some erroneous points outside the general body of the scanned surface due to the errors introduced by the IMU or RTK-DGPS. A point cloud segmentation approach using connected component labeling (in CloudCompare v2) using an 8th level octree and 10,000 connected points in the primary segment was used to remove these errors.

The pre-processed point cloud result is shown in Fig. 2(b).

2.3 Processing workflow

The following processing steps were applied to the pre-processed point cloud:

Height filtering: the point cloud returns were filtered into ground and vegetation classes using the BCAL height filtering tool [6] with a canopy spacing of 5 m and maximum vegetation height of 30 m.

LiDAR metrics: A total of 35 LiDAR metrics related to vegetation (such as maximum height, vegetation density, kurtosis, foliage height density, etc.), topography (such as local roughness, slope sine aspect, etc.) and intensity (such as intensity mean, standard deviation, etc.) were derived at a grid resolution of 0.1 m using the BCAL tool [7].

Dimensionality reduction: a large number of LiDAR metrics generated in the process does not necessarily contain useful information. Two data transformation techniques – principal component analysis (PCA) [8] and independent component analysis (ICA) [9] were used to condense the information content of 35 LiDAR metrics (treated similar to hyperspectral bands) to 15 LiDAR metrics, where the eigenvalues > 0.2 .

Spatial filtering: a 3x3 enhanced frost filter [10] was used to adaptively average pixel values in homogenous clusters with a coefficient of variation, C_u=0.523 and uses an impulse response convolution kernel for heterogeneous clusters with a maximum coefficient of variation, C_{max}=1.732.

Classification: a set of 7 classifiers – Parallelepiped (PP), Maximum Likelihood (ML), Minimum Distance (MD),

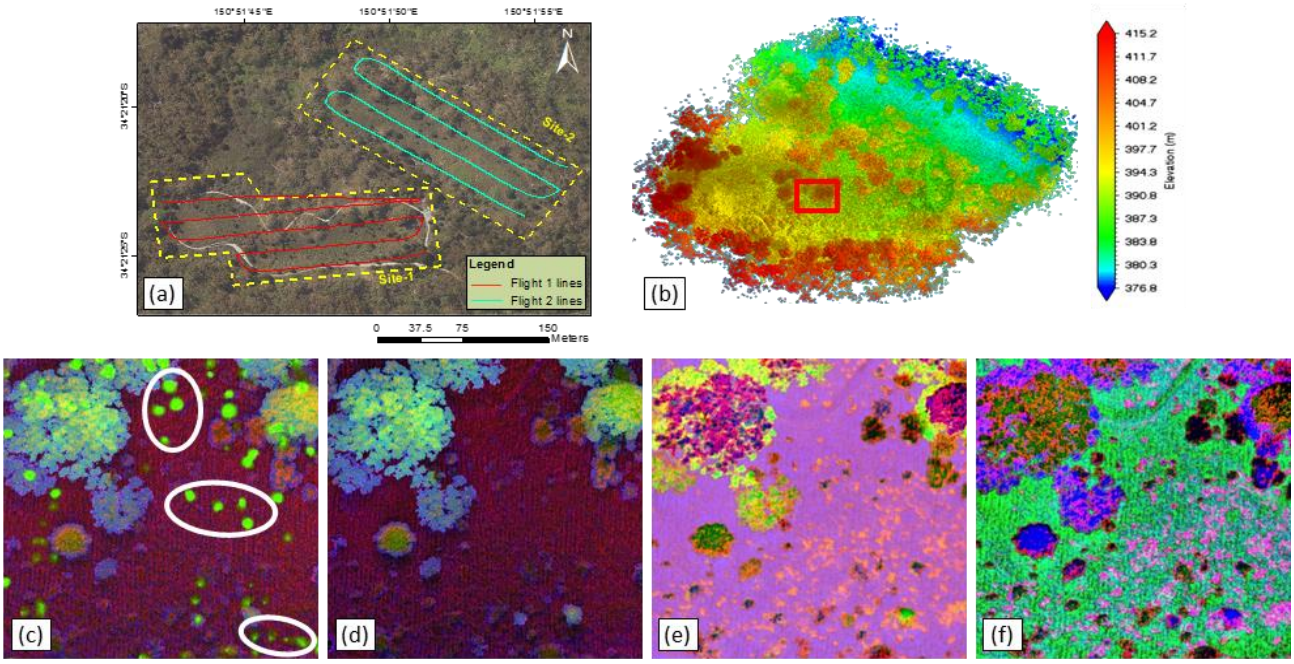

Fig. 2.(a) UAV-LiDAR flight lines for Site-1 and Site-2; (b) pre-processed point cloud (colorised as per elevation); false color composite (kurtosis, maximum vegetation height, and coefficient of variation) of lidar matrices (c) without pre-processing and (d) with pre-processing; and false color composite (of first three layers) of data transformed with (e) PCA and (f) ICA

Mahalanobis Distance (MHD), Spectral Angle Mapper (SAM), Spectral Information Divergence (SID), and Support Vector Machine (SVM) were evaluated to classify the PCA and ICA data into swamp and and non-swamp vegetation classes.

Fusion: in addition, to the transformed LiDAR matrices (PCA and ICA), high-resolution (7.5 cm spatial resampled to 0.1 m) optical data were stacked with the 35 LiDAR matrices (at 0.1 m) and then transformed to form two dimensionally reduced composites (RGB+PCA and RGB+ICA). These composites were also evaluated using the set of 7 classifiers.

3. RESULTS AND DISCUSSION

Fig. 2(b) shows the synoptic overview of the pre-processed point cloud. Fig. 2(c)-(d) displays a false colored composite (FCC) of the processed LiDAR matrices (kurtosis, maximum vegetation height, and coefficient of variation) for a spatially subset region marked by a red rectangle in Fig. 2(b). Pre-processing is essential to avoid erroneous artifacts in the processed FCC of the LiDAR metrics (as marked in white in Fig. 2(c)); such artifacts are removed with pre-processing, as shown in Fig. 2(d). Fig. 2(e) and (f) show the FCC of the first three bands of the transformed LiDAR matrices using PCA and ICA, respectively. The sampled ground truth points (320) and polygons (128) were randomly divided into 1:1 sets of ground truth training and test samples, with 160 points and 64 polygons each. The ground truth training set was used to train the classifiers and the test samples were used to compute the overall accuracy (*OA*), kappa (*k*) and confusion matrix to evaluate the classification accuracies. Table 1 lists the *OA* and *k* of classification accuracy achieved with PCA, ICA, RGB+PCA and PGB+ICA datasets using the 7 different classifiers. SVM achieved the highest *OA* and *k* for each dataset. The accuracy was slightly improved when RGB bands were used along with the LiDAR matrices as in case of RGB+PCA and PGB+ICA with SVM, highlighting the benefit of the added spectral information.

Table 1 Accuracy assessment for the classification

Classifier		PCA		ICA		RGB+PCA		RGB+ICA	
		OA(%)	*k*	*OA(%)*	*k*	*OA(%)*	*k*	*OA(%)*	*k*
PP		14.0	0.11	04.9	0.36	10.6	0.08	04.4	0.03
ML		53.3	0.46	53.8	0.46	54.8	0.48	57.8	0.51
MD		35.2	0.27	53.7	0.46	36.2	0.26	64.9	0.58
MHD		47.3	0.39	55.8	0.48	46.8	0.38	67.5	0.61
SAM		35.3	0.27	53.7	0.46	36.5	0.27	62.7	0.55
SID		35.5	0.27	35.9	0.27	38.1	0.28	56.7	0.49
SVM		**68.9**	**0.62**	**69.9**	**0.61**	**70.5**	**0.63**	**73.6**	**0.67**

Fig. 3. shows the output classification map of the SVM classifier on RGB+ICA dataset. The corresponding producer's and user's accuracy for each class is listed in Table 2. Overall the accuracy for each class is satisfactory; particularly to differentiate between swamp type (Sedgeland complex) and non-swamp type (Eucalyptus) vegetation. Furthermore, the results also indicate the potential of the

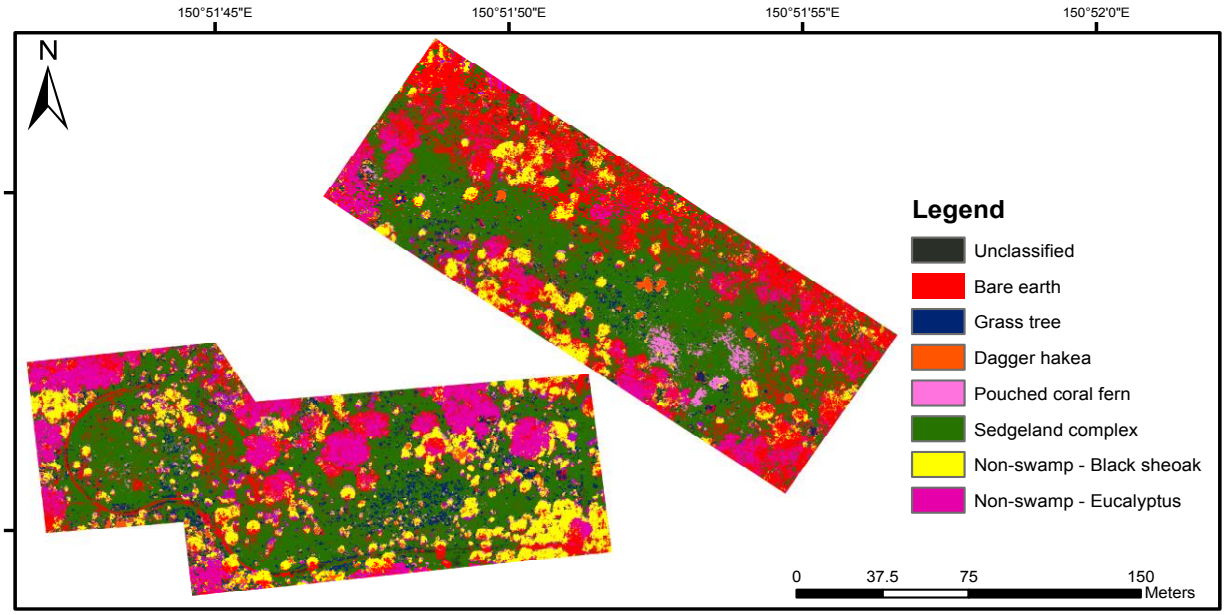

Fig. 3. Output classification produced by RGB+ICA using SVM

process to distinguish between certain swamp type (Grass tree, Dagger Hakea, and Pouched coral fern) and non-swamp type (Black sheoak) species.

Table 2 Accuracy assessment for the classification

Class	*Prod. Acc. (%)*	*User Acc. (%)*
Bare earth	31.0	82.8
Grass tree	20.1	52.3
Dagger Hakea	97.7	93.5
Pouched coral fern	54.7	86.2
Sedgeland complex	89.5	72.0
Non-swamp - Black sheoak	81.1	83.7
Non-swamp - Eucalyptus	65.1	83.0

4. CONCLUSION

This study showed the benefits of high-resolution LiDAR data obtained from a UAV-LiDAR system. The derived LiDAR matrices can be transformed using methods such as PCA and ICA to efficiently employ classification algorithms such as SVM. The accuracy increased with the addition of RGB layers in the classification workflow, this indicates the potential of fusion with other high-resolution data such as hyperspectral data obtained from UAVs to further improve the classification accuracy.

5. REFERENCES

[1] NNPWS., *The native vegetation of the Woronora, O'Hares and Metropolitan Catchments.* NSW National Parks and Wildlife Service, Sydney, 2003.

[2] Jenkins, R.B. and P.S. Frazier, *High-resolution remote sensing of upland swamp boundaries and vegetation for baseline mapping and monitoring.* Wetlands, 2010. **30**(3): p. 531-540.

[3] Strecha, C., et al., *Developing species specific vegetation maps using multi-spectral hyperspatial imagery from unmanned aerial vehicles.* ISPRS Annals of the Photogrammetry, Remote Sensing and Spatial Information Sciences, 2012. **3**: p. 311-316.

[4] Lechner, A., et al., *Characterising Upland Swamps Using Object-based Classification Methods and Hyper-spatial Resolution Imagery Derived from an Unmanned Aerial Vehicle.* ISPRS Annals of the Photogrammetry, Remote Sensing and Spatial Information Sciences I-4, 2012: p. 101-106.

[5] Banerjee, B.P., S. Raval, and P.J. Cullen, *High-resolution mapping of upland swamp vegetation using an unmanned aerial vehicle-hyperspectral system.* Journal of Spectral Imaging, 2017. **6**(1): p. 1-6.

[6] Streutker, D.R. and N.F. Glenn, *LiDAR measurement of sagebrush steppe vegetation heights.* Remote Sensing of Environment, 2006. **102**(1): p. 135-145.

[7] BCAL Lidar Tools for ENVI 5.3. Boise State University, Department of Geosciences, 1910 University Drive, Boise, Idaho. URL: http://bcal.boisestate.edu/tools/lidar

[8] Richards, J.A. and J. Richards, *Remote sensing digital image analysis*. Vol. 3. 1999: Springer.

[9] Hyvärinen, A. and E. Oja, *Independent component analysis: algorithms and applications.* Neural networks, 2000. **13**(4): p. 411-430.

[10] Lopes, A., R. Touzi, and E. Nezry, *Adaptive speckle filters and scene heterogeneity.* IEEE transactions on Geoscience and Remote Sensing, 1990. **28**(6): p. 992-1000.